TECHNICAL DOCUMENTS LIAISON OFFICE
UNEDITED ROUGH DRAFT TRANSLATION

THE ATOMIZATION OF LIQUID FUEL BY MEANS OF PNEUMATIC INJECTORS

BY: L. A. Vitman, B. D. Katsnel'son and M. M. Efros

English Pages: 39

SOURCE: Voprosy Aerodinamiki i Teploperedachi v Kotel'no-Topochnykh Protsessakh, Moskva, 1959, pp. 5-34

THE ATOMIZATION OF LIQUID FUEL BY MEANS OF PNEUMATIC INJECTORS

L. A. Vitman, B. D. Katsnel'son, and M. M. Efros

Introduction

The combustion of liquid fuel in an air stream occurs in several successive stages: evaporation, pyrogenic decomposition, and combustion. These stages are preceeded by atomization, the qualities of which determine, to a considerable extent, the intensity of the evaporation.

Masut and other types of liquid fuels are atomized by means of injectors, which can be divided into two main groups - mechanical and air (or steam) injectors. The latter can, in turn, also be divided into two groups - high- and low-pressure.

Such a categorization is arbitrary. When the atomization agent has a pressure up to 1000 mmHg, the injectors usually belong in the low-pressure category, while with pressures greater than 1000 mmHg, they are usually high-pressure. While many studies have been devoted to mechanical injectors, very little has been done concerning air atomizers, particularly low-pressure ones [1-7].

Certain authors [8, 9, etc.] assume that the stream breaks up

because of external forces on its surface. The surface tension of the liquid counteracts the external forces which are determined by the energy of the flux.

Other researchers [10,11] have determined the stream breakdown, starting with the conditions of disruption of the equilibrium of the free surface of the liquid, under the effect of surface tension. Slight initial disturbance of the surface leads to the formation of waves; the amplitude of certain of these increases with time, resulting in breakdown of the stream of liquid. When there is considerable relative speed between the liquid and air streams, additional disturbances occur, caused by the action of external forces on the fuel jet.

On the basis of the capillary wave theory, Rayleigh [10] determined the conditions for the breakdown of a stream of inviscid liquid. G. I. Petrov and T. D. Kalinina solved an analogous problem, taking into account the effect of the air on the fuel jet.

K. Weber [11] determined analytically the breakdown conditions and the length of the continuous part of a stream of viscous liquid, also applying the theory of slight oscillations to this case. For a liquid jet with viscosity μ, coefficient of surface tension α, and density ρ_1, emerging from a round orifice of radius R_0 into a stream of inviscid gas of density ρ_g with relative velocity $\underline{w}$ considerably less than the speed of sound, we have the following equation for the dependence of the oscillation increment on wave number ξ:

$$q^2 + q\frac{3\mu}{\rho_1 R_0}\xi^2 = \frac{\alpha}{2\rho_1 R_0^3}(1-\xi^2)\xi^2 + \frac{\rho_g w^2 \xi^3}{2\rho_1 R_0^2}\varphi_0(\xi). \qquad (1)$$

Analysis of this expression makes it possible to isolate those oscillations which lead to jet decay. These oscillations should have

corresponding positive q-values. In this case, the maximum q-value will describe the oscillation which most rapidly leads to jet decay. However, Weber did not carry equation (1) to its solution applicable in practice; in particular he did not determine the mean drop size, which is of greatest technical interest.

At the present time, it is very difficult to give a complete analytical solution of the problem of drop sizes.

First, to solve the problem of which of the unstable oscillations, under the given conditions, leads to decay, it is necessary to know the wavelength and the intensity of the oscillations in the jet. These oscillations are given by the initial conditions of jet injection, i.e., by the nature of the jet flow in the injector, the atomizer design, the processing and the state of the surface of the nozzle, etc.

Second, the obtained drops are the result of the complex process of the breakdown of the drops which first form. This latter process might be expressed by the equation of pulsational motion and the boundary conditions which correspond to the intermediate state of the drops. However, it is impossible to formulate the boundary conditions for the intermediate stages, since it is impossible to trace all the changing shapes of jet decay. Thus, the given system excludes the possibility of a complete analytical solution of the problem. Nevertheless, it is possible, from the equation for jet instability, to derive similitude criteria which describe the atomization process. If we consider that with process similitude there should be preserved, in the same manner, the relationships between oscillation wavelength and the diameters of the obtained drops, on the basis of the experiment we should obtain a form of the

functional relationship between the criteria. This makes it possible to determine the mean drop size.

In studying the atomization of a liquid by air or vapor injectors, B. D. Katsnel'son and V. A. Shvab [12], from an examination of the movement of a drop in a stream of gas (vapor), used the theory of similitude for generalized experimental data, and obtained a relationship which made it possible to determine mean drop size when the viscosity of the liquid does not effect the atomization.

Let us use equation (1) to obtain similitude criteria for the atomization of a viscous liquid. Using the π-theorem, after dropping the constants and replacing ξ by $-\frac{2\pi R_0}{\lambda}$, we get the following complexes:

$$\left.\begin{array}{ll} 1)\ q^2\frac{\rho_1 R_0^3}{\alpha}\left(\frac{\lambda_1}{R_0}\right)^2; & 3)\ \frac{R_0}{\lambda_1}; \\ 2)\ q\frac{\mu R_0}{\alpha}; & 4)\ \frac{\rho g w^2 R_0}{\alpha}\cdot\frac{R_0}{\lambda_1}. \end{array}\right\} \qquad (2)$$

Analysis of the values appearing in these complexes shows that λ_1 and q are functions of the process. It must be noted that the value q appearing in the criteria is inversely proportional to the time T from the moment the jet emerges from the atomizer until it begins to decay, and describes the rate of growth of the amplitude of the disturning oscillations. Consequently, instead of q we can write $\frac{1}{T}$.

After certain transformations, we get the following criteria:*

$$\left.\begin{array}{ll} \Pi_1=\frac{\mu^2}{\rho_1\alpha D}, & \Pi_2=\frac{\rho w^2 D}{\alpha}, \\ \Pi_3=\frac{D}{\lambda_1}, & \Pi_4=\frac{\mu}{\rho_g w^2 T}, \end{array}\right\} \qquad (3)$$

*When writing the criteria, we use diameter $D = 2R_0$ instead of the radius R_0 as the dimension to be determined.

where μ is the coefficient of viscosity of the liquid; ρ_1 is the density of the liquid; α is the coefficient of surface tension; D is the characteristic geometric size of the injector; ρ_g is gas density; w is the relative speed between the air and the liquid; λ_1 is the wavelength of the oscillation at which the jet begins to decay into drops; and T is the time from the moment the jet emerges from the nozzle until it begins to decay into drops.

Of the obtained criteria, Π_1 and Π_2 are definite, while Π_3 and Π_4, containing the values λ_1 and T, are indefinite.

Since the present article* does not treat the dynamics of the process of jet decay, but merely gives the final results, there is no need of including criterion in the functional dependence. Thus, the atomization process can be described by the dependence

$$\frac{D}{\lambda_1} = f\left(\frac{\mu^2}{\rho_1 \alpha D};\ \frac{\rho_g w^2 D}{\alpha}\right). \qquad (4)$$

Assuming that for similar processes λ_1/d = idem, where d is the mean drop diameter, we can introduce, instead of the criterion D/λ_1, the criterion D/d into the examination, or its inverse value, i.e., d/D. Then the functional connection between the criteria becomes

$$\frac{d}{D} = f\left(\frac{\mu^2}{\rho_1 \alpha D};\ \frac{\rho_g w^2 D}{\alpha}\right). \qquad (5)$$

The criterion $\frac{\mu^2}{\rho_1 \alpha D}$ describes the relationship of the forces of viscous, inertial, and surface tensions.

The criterion $\frac{\rho_g w^2 D}{\alpha}$ describes the relationship of the inertial forces of an air stream to forces of surface tension, i.e., it takes

---

*The present work was done under the direction of Professor I. I. Paleyev. Later, A. S. Lyshevskiy, also under Paleyev's direction, applied the basic results of this work to a study of atomization by pressure injectors.

into account the interaction of the deforming jet with the external medium.

The criterion d/D gives the relationship between the mean drop diameter and the characteristic size, and determines the degree of dispersion of the flame.

When the values of the viscous forces of a liquid are small compared with the inertial and surface tension forces, the decay process will be defined by the criterion $\frac{\rho_r w^2 D}{\alpha}$ alone. In this case, equation (5) is simplified and assumes the form:*

$$\frac{d}{D} = f\left(\frac{\rho_r w^2 D}{\alpha}\right). \qquad (5')$$

The numerical values of the coefficients in equation (5) can vary as the initial conditions of jet injection which, in turn, are described by the features of various injector designs. However, the form of the functional connection between the criteria remains unchanged for various injectors.

It must be pointed out that this dependence does not consider the braking of the gas flow by the fluid jet, since the initial relative velocity enters into the criteria. The change in the rate in the atomization process will vary, depending on the value of the criterion $\frac{\mu}{\rho_g w^2 T}$, which describes the decay time, and depending on the relationship of the amount of gas and liquid. However, this problem is not examined in the present article, since this factor had no essential significance in the investigated regimes.**

---

*In Rayleigh's solution, which treats the decay of an inviscid fluid in the absence of the effect of external forces, the value d/D is constant.

**For more on this, see the work by L. A. Vitman in the present collection.

1. Study of the Atomization of a Viscous Fluid on a Laboratory Installation

The determination of the influence of viscosity on the fineness of atomization of a liquid has great value in industry. Let us mention the work of L. K. Ramzin [9], who, in his experiments, detected no dependence whatsoever between fineness of atomization and the viscosity of the liquid, although the latter was measured from approximately 2 to 23°E.

V. F. Kopytov has described the results of experiments on the comparison of masut in an oven with low-pressure injectors. In this work it was noted that a decrease in the viscosity of the masut from 52 to 9.2°E has no significant effect on combustion.

I. V. Astakhov, in his study of mechanical high-pressure injectors, experimented with liquids having various viscosities - from 3.82 to 13.5°E. Although in his final formula for determining fineness of atomization the author did not consider the viscosity of the fuel, the experimental diagrams and tables show a definite dependence of the average diameter of the forming drops on the coefficient of viscosity.

We conducted special experiments in order to study the influence of viscosity on the degree of dispersion of fuel.

Figure 1 gives a diagram of the experimental installation. The working liquid, under air pressure, is removed from measuring buret 1, which served as the fuel tank, and is fed through tube 2 to air atomization injector 3. The air from compressor 4 is fed through compensating tank 5, after which it splits, passing through tap 6 and unit 7 to the injector orifice for atomization, and through tap 8 to fuel tank 1 for transporting the liquid. The air flow-rate is

measured by rheometer 9, and the air pressure is measured by manometers 10, 11 and 12. The liquid consumption is determined from graduated buret 1, which has a volume of 200 cc. The reading accuracy is within 1% (2 cc).

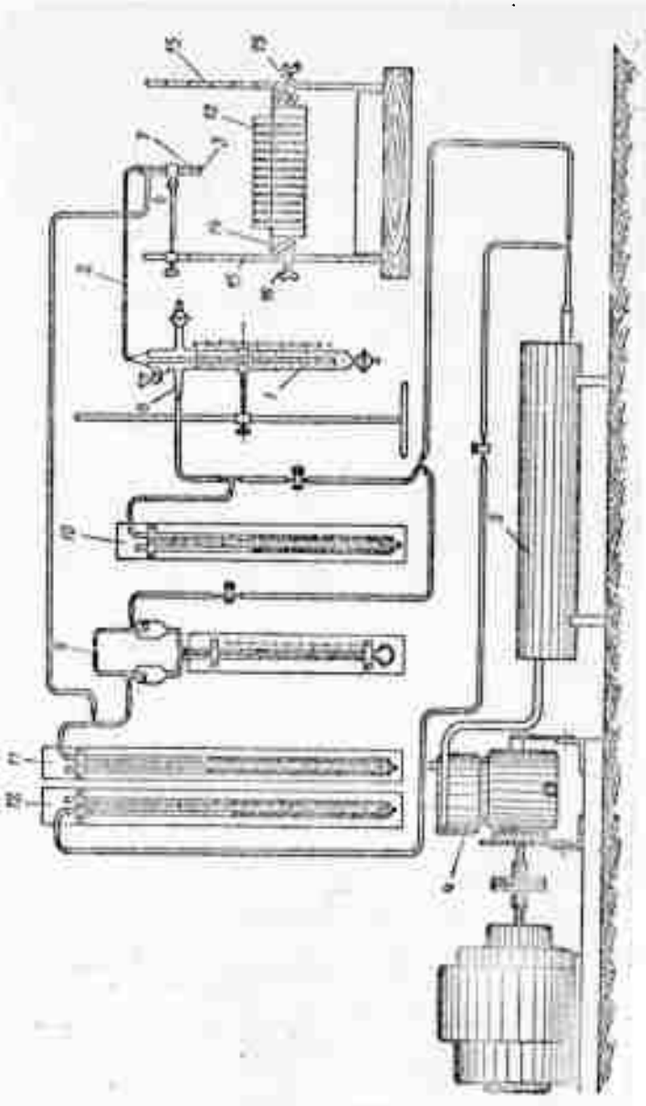

Figure 1. Diagram of the experimental installation for determining the influence of viscosity on the fineness of atomization of a liquid.

The distribution of the liquid through the cross section of the atomized jet is determined by graduated cylinders 13 attached to frame 14 which can be adjusted for height on stand 15 and fastened at a specific level by clamps 16. Using this, it was possible to determine the fuel distribution by jet cross section at various heights, i.e., at various distances from the injector orifice. The amount of liquid in the graduated cylinders was determined by weighing on an analytical balance. The drops were collected on smoked glass and measured with a 56-power microscope. For instantaneous cut-off of the drops we used a specially designed instrument, operating on the principle of a corkscrew seal.

The installation was made entirely of glass. The injector orifice was in the form of two concentric openings: the atomized liquid was fed through the inner opening, and air was fed through the outer (ring-shaped) opening. The diameter of the exhaust cross section for the liquid D = 0.506 mm and, accordingly, the area $F = 0.201$ mm^2. For the ring-shaped cross section (for the air), $F = 2.9$ mm^2.

Measurements were made at varying distances along the jet, in order to determine the degree of dispersion and the density of the flame. The least distance between the measurement point and the injector was 75 mm. Attempts to perform the experiments at a closer distance were unsuccessful, since it was impossible to obtain cross-sectional fuel distribution at the base of the flame, while the high speed of the jet made it impossible to cut off and collect the drops. The slides, covered with soot, on which the drops were collected, were set up at thirty places along the diameter of the jet, corresponding to the geometric position of the graduated cylinders. The

obtained discrete diameters of the drops of each sector had characteristic atomized mass, determined by the density of the spraying and the area of the respective half-ring sector.

The mean diameter of the drops was found from the formula

$$d = \frac{\sum_{i=1}^{n} g_i d_i}{\sum_{i=1}^{n} g_i}, \qquad (6)$$

where g_1 is the total weight of drops of diameter d_i.

It should be pointed out that the mean diameter of the drops is an arbitrary value, since the jet actually contains an enormous number of drops with varying sizes. However, the mean diameter reflects, to a known degree, the nature of the atomization, which is determined by the hydrodynamic peculiarities of the process, the physical properties of the liquid, and the geometric dimensions of the injectors.

The discrete values of the collected drops were calculated in 25μ -intervals, and determined as the arithmetic mean. For example, for drops from 0-25μ, d_1 = 12.5; for drops 25-50μ, d_1 = 37.5μ, etc. If the relative error for small drops is relatively high, as the size increases the relative error decreases, becoming insignificant for large diameters. This is quite important in determining $\underline{d}$ from formula (6), since small drops, no matter how many, have an insignificant effect on the absolute magnitude of the averaged diameter.

Description of the Experiments, and the Results of Their Reduction

Table 1 gives a list of the liquids used, and their physical properties.

Table 1

Characteristics of the liquids

series number	liquid	specific weight kg/m³	viscosity μ kg·sec/m² · 10^{-3}	viscosity μ °E	surface tension σ, kg/m · 10^{-3}
I	solution of glycerine and water	1250	54,500	59,00	6,45
II	The same	1240	20,200	31,50	6,49
III	» »	1230	16,300	18,00	6,53
IV	» »	1210	6,050	7,00	6,61
V	» »	1185	2,400	3,00	6,72
VI	» »	1120	0,560	1,30	7,18
VII	kerosene	815	0,308	1,15	2,80
VIII	gasoline	745	0,067	0,99	2,39

As Table 1 shows, the working liquids differed in surface tension approximately by a factor of three: from $7.18 \cdot 10^{-3}$ to $2.39 \cdot 10^{-3}$; the viscosity, however, varied from 60 to 1°E.

Nineteen experiments were conducted in Series I. The liquid flow-rate varied from G = 0.48 to G = 2 kg/hr; the air flow-rate varied from L = 0.45 to L = 1.26 m^3/hr. The ratio of air to fuel L'/G = 0.27 - 3.15 kg/kg, where L' is the air flow-rate in kg/hr. The air speed w_g = 43 - 121 m/sec, and the speed of the liquid w_l = 0.55 - 2.3 m/sec, so that the relative velocity $w = w_g - w_l$ is determined, essentially, by the speed of the air stream. The air pressure at the injector orifice varied from 54 to 550 mmHg.

The experiments were conducted at four distances along the jet: 75, 125, 200 and 275 mm from the injector orifice.

Figure 2 shows the curves of the distribution of atomized liquid throughout the jet, typical of the remaining series. The abscissa contains the distances r from the center of the jet 0 to the center of the graduated cylinder, in millimeters, while the ordinate contains the weight of the liquid per unit area of the collecting vessels g/f, in percents. As the diagram shows, the greatest density occurs in the center of the jet, with symmetrical drop at the edges.

Such distribution is characteristic of air-atomization injectors.

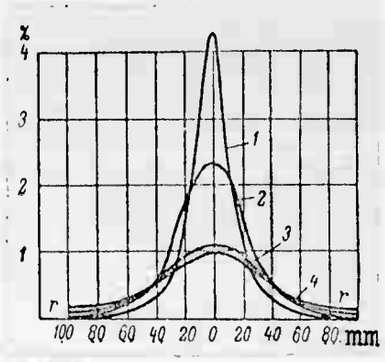

Figure 2. Distribution of atomized liquid throughout the jet for various distances from the injector orifice. 1) 75 mm; 2) 125 mm; 3) 200 mm; 4) 275 mm.

The relationship $\frac{d}{D}=f\left(\frac{\rho_a w^2 D}{\sigma}\right)$, constructed in Fig. 3 in logarithmic anamorphism, connects with a straight line all points of the experiments of this series, and can be expressed by the equation

$$\frac{d}{D}=A\left(\frac{\rho_a w^2 D}{\sigma}\right)^{-0,45}, \qquad (7)$$

where A = 2.4.

In this figure, the different designations pertain to experiments conducted for various distances from the injector orifice.

Since in the experiments of Series I and IV the measurements were made at four distances from the injector orifice, and showed no noticeable change with regard to the fineness of atomization, the other series investigations were made mainly (except for the controls) at one level - 200 mm from the injector. The points of the experiments of all remaining series, as Series I, were on corresponding straight lines, which can be expressed by a formula analogous to (7), but with differing numerical coefficients A. Table 2 gives the values of these

coefficients.

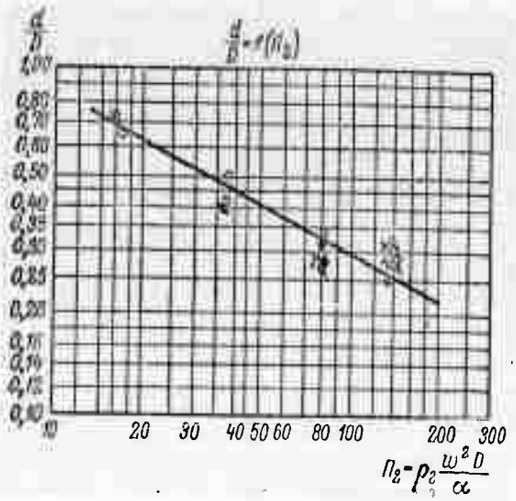

Figure 3. The function $\frac{d}{D} = f\left(\frac{\rho\omega^2 D}{\alpha}\right)$ for the experiments of Series I.

Table 2

Values of Coefficients A in formula (7).

Values of Coefficients A in formula (7)

Series	I	II	III	IV	V	VI	VII	VIII
A	2,40	1,90	1,60	0,95	0,85	0,77	0,77	0,77

The exponent n was identical for all the experimental series, while the coefficients A were identical in the last three series (VI, VII, VIII), where the working liquid was a mixture of glycerine and water with a viscosity of 1.3°E, kerosene with a viscosity of 1.15°E, and gasoline with a viscosity of 1°E. In the constructed dependence

$$\frac{d}{D} = f\left(\frac{\rho\omega^2 D}{\alpha}\right)$$

the experimental points of all three series are grouped about one straight line, as shown in Fig. 4.

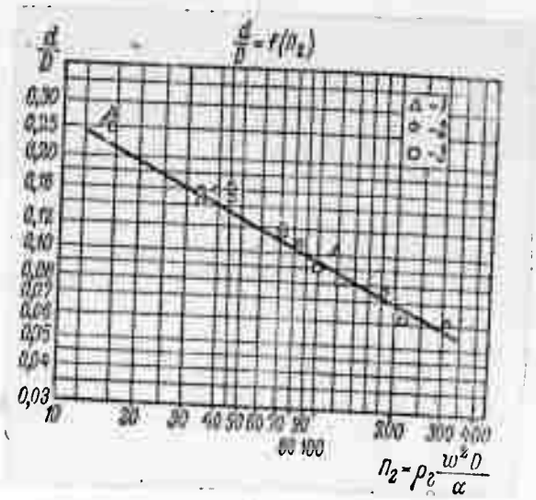

Figure 4. The function $\frac{d}{D}=f\left(\frac{\rho_2 w^2 D}{\sigma_a}\right)$ for Series VI, VII, and VIII. 1) $\frac{\mu^2}{\rho_1 \sigma D}=6\cdot10^{-4}$; 2) $\frac{\mu^2}{\rho_1 \sigma D}=8\cdot10^{-4}$; 3) $\frac{\mu^2}{\rho_1 \sigma D}=5\cdot10^{-5}$

An examination of the experiments shows that the atomization process for each liquid, in accordance with the theoretical analysis, has a well-defined functional connection

$$\frac{d}{D}=A\left(\frac{\rho_2 w^2 D}{\sigma_a}\right)^{-0,45}. \qquad (7')$$

encompassing a range of viscosity changes from 1 to 60°E, and the viscosity influences the value of the coefficient A (see Table 2).

As has already been shown above, the influence of viscosity forces on atomization is described by the criterion

$$\frac{\mu^2}{\rho_1 \sigma D}.$$

If we construct, in semi-logarithmic anamorphism, the function

$$\frac{d}{D}\left(\frac{\rho_2 w^2 D}{\sigma_a}\right)^{0,45}=f\left(\frac{\mu^2}{\rho_1 \sigma D}\right), \qquad (8)$$

as can be seen from Fig. 5, all the experimental data are described

by a single curve. This curve can be expressed approximately by the following formulas:

when $\frac{\mu^2}{\rho_1 \sigma D} < 0{,}5$

$$\frac{d}{D}\left(\frac{\rho_g w^2 D}{\sigma}\right)^{0,45} = A_0 + 1{,}24\left(\frac{\mu^2}{\rho_1 \sigma D}\right)^{0,62}, \qquad (9)$$

when $\frac{\mu^2}{\rho_1 \sigma D} > 0{,}5$

$$\frac{d}{D}\left(\frac{\rho_g w^2 D}{\sigma}\right)^{0,45} = A_0 + 0{,}94\left(\frac{\mu^2}{\rho_1 \sigma D}\right)^{0,28}; \qquad (9')$$

for the given injector, $A_0 = 0.77$.

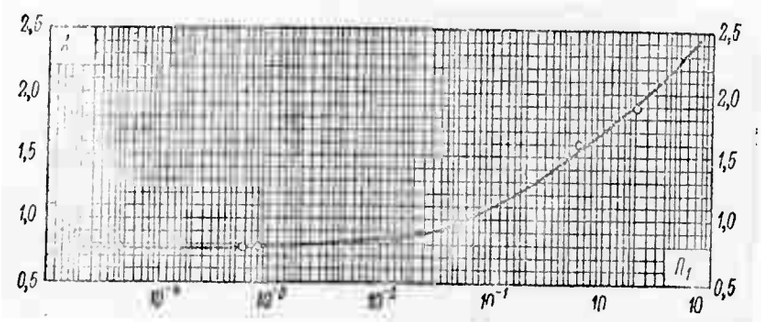

Figure 5. The function $\frac{d}{D}\left(\frac{\rho_g w^2 D}{\sigma}\right)^{0,45} = f\left(\frac{\mu^2}{\rho_1 \sigma D}\right)$

The formulas derived hold for values of the criterion $\frac{\mu^2}{\rho_1 \sigma D}$ from $4.5 \cdot 10^{-5}$ to 7.25, and for values of $\frac{d}{D}\left(\frac{\rho_g w^2 D}{\sigma}\right)^{0,45}$ from 0.77 to 2.4.

From Fig. 6 it is evident that viscosity begins to have an essential influence on the fineness of atomization when the criterion $\frac{\mu^2}{\rho_1 \sigma D}$ has values greater than 10^{-1}.

The two computational graphs (Figs. 6 and 7) have been constructed for graphic representation of the influence of the coefficients of viscosity and surface tension on the fineness of atomization. Both graphs were calculated from the above-given formulas.

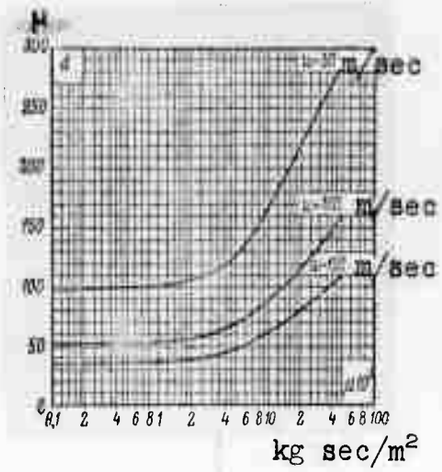

Figure 6. Average diameter of the forming drops vs. viscosity at various speeds, presupposing that the coefficient of surface tension of the liquid, the air density, and the geometric dimensions of the injector, are constant.

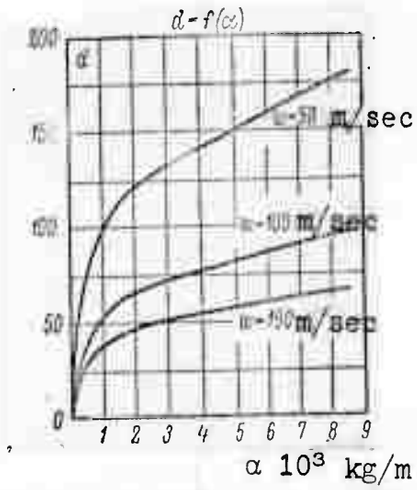

Figure 7. Average diameter of the forming drops v. the coefficient of surface tension at various speeds, presupposing that the viscosity of the liquid, the gas density, and the geometric dimensions of the injector, are constant.

Figure 6 gives the average diameter of the forming drops vs. viscosity $d = f(\mu)$ at various speeds, assuming that all other values

in the formula: the coefficient of surface tension, density, and geometric size, are constant.

Figure 7 shows a graph which gives the average diameter of the drops vs. the coefficient of surface tension of the liquids $d = f(\alpha)$ at various speeds, assuming that all the other factors: viscosity and geometric dimensions, are constant.

The combustion of masut under industrial conditions is usually preceded by its heating. In this case the viscosity has practically no effect on the fineness of atomization. Let us determine the value of the mean diameter of the drops vs. the dimensions of the injector nozzle, and the relative flow rate. For this, let us use formula (7'), slightly transformed. The coefficient of surface tension of masut is $\sim 3.5 \cdot 10^{-3}$ kg/m; the density of the atomized air is taken as 0.12 kg $\cdot$ sec^2/m; then,

$$\frac{d}{D} = A\left(\frac{0{,}12w^2D}{3{,}5\cdot 10^{-3}}\right)^{-0{,}45}, \qquad (10)$$

$$d = 0{,}204A\frac{D^{0{,}55}}{w^{0{,}9}}. \qquad (10')$$

Sometimes it is interesting to express the average drop diameter by the air flow-rate. Since the speed of masut is considerably less than that of an air stream, we can consider, approximately, that

$$w = w_{air},$$

and then,

$$L_{air} = w\frac{\pi D^2}{4}\cdot 3600,$$

$$d = 258A\frac{D^{2,35}}{L^{0,9}}. \qquad (11)$$

We must state that within the limits of our experiments we noted no essential change in the atomization quality as a function of the

air and liquid flow-rate ratio. We can assume that with other ratios L/G the influence of the latter begins to be felt, and this requires special study.

We must also turn our attention once again to the fact that in the experiments we were not able to discern a change in drop diameter along the jet. This can be seen from Fig. 3, which contains the results of measurements at four different heights, beginning 75 mm from the injector. We can conclude that the drop breakdown process terminates at a very small sector after the fuel encounters the air. There is some doubt as to the assertion made by individual scientists to the effect that drops enlarge with an increase in distance from the injector along the jet [13].

2. A Study of Industrial Injectors

In all, we tested five basic types of injectors: the STS-FDB-1, the STS-FOB-2, the STS-FDM-1, the Glushakov injector, and the two-stage injector. Tests with the STS-FOB-2 injector were conducted using three additional inserts and five nozzles in various combinations.

The STS-FDB-1 injector (Fig. 8) operates on the "dual control" principle. All the air required for combustion enters through tube 1 and braches into two streams - the primary and the secondary. The primary air stream is fed through channel 2 (constant cross section) against the jet of fuel entering through tap 3 into tube 4. The gas-liquid mixture enters expansion insert 5 and at a certain distance, at almost right angles, encounters the second air stream, the amount of which is controlled by the variable cross section of anular channel 6. Valve 7 serves to control the total air flow-rate.

Table 3

Results of experiments with a laboratory injector

liquid flow-rate G, kg/hr;	air flow-rate L, m^3/hr;	average drop diameter $\underline{d}$, μ;	distance from injector orifice $\underline{h}$, mm;
Series I			
0.55	1.26	150.2	275
0.48	1.26	153.1	200
0.55	1.26	142.3	125
0.96	1.26	151.1	275
0.87	1.26	153.0	200
0.87	1.26	152.6	125
0.79	1.26	143.0	75
0.64	1.26	131.7	75
0.69	0.97	143.5	275
0.73	0.97	172.7	200
0.89	0.97	159.6	125
0.98	0.97	140.0	125
0.89	0.97	144.0	75
1.13	0.97	148.8	200
1.30	0.67	206.0	125
1.13	0.67	212.0	200
0.73	0.67	253.0	200
2.02	0.45	358.6	125
0.84	0.45	326.0	200
Series II			
1.20	1.26	117.7	200
1.26	0.97	146.8	200
1.33	0.97	142.5	200
1.15	0.67	170.3	200
1.06	0.67	154.4	200
1.15	0.45	253.9	200
0.81	0.45	242.3	200
Series III			
1.33	1.26	98.0	200
1.09	0.97	120.0	200
1.37	0.97	113.4	200
0.84	0.67	138.5	200
0.75	0.45	196.5	200
1.13	0.45	221.6	200
Series IV			
1.27	1.26	45.6	275
1.16	1.26	47.8	200
1.03	1.26	53.6	125
1.02	1.26	53.6	75
1.14	0.97	68.6	200
0.70	0.67	89.4	275
1.41	0.67	89.1	200
1.18	0.67	97.9	50
0.61	0.45	139.5	200
0.82	0.45	156.2	200
Series V			
1.96	1.26	48.7	200
1.43	0.97	73.2	200
1.35	0.97	78.0	200
0.684	0.67	78.1	200
0.452	0.45	120.5	200
0.452	0.45	102.5	200
Series VI			
0.57	1.26	50.7	200
1.38	1.26	42.3	200
0.88	0.97	60.8	200
1.15	0.97	58.7	200
0.81	0.67	77.6	200
0.96	0.67	74.0	200
2.13	0.45	130.4	200
0.61	0.45	139.5	200
0.68	0.45	126.6	200
Series VII			
1.05	1.26	30.8	200
1.04	0.97	38.2	200
0.817	0.67	55.1	200
0.44	0.45	81.2	200
Series VIII			
1.00	0.97	32.4	200
0.69	0.67	45.8	200
0.47	0.45	82.1	200
0.45	0.45	75.0	125

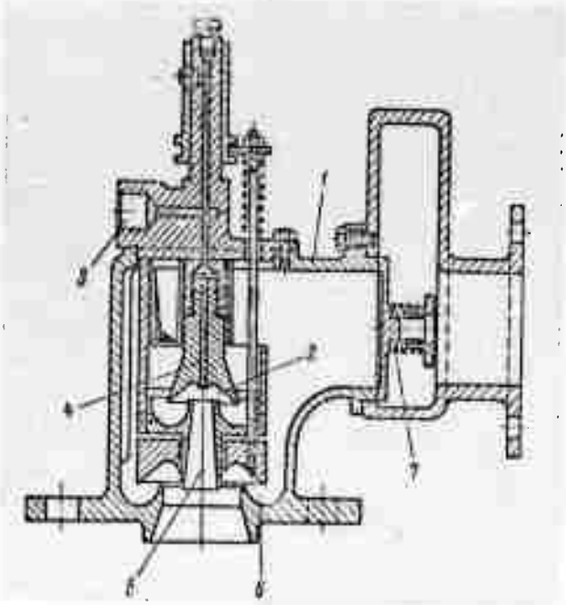

Figure 8. Cut-away view of the STS-FDB-1 injector.

The STS-FOB-2 (ROMO) [Republic General Machinery Association] injector (Fig. 9) consists of housing 1 with central tube 2 through which the fuel enters. The air is fed through pipe 3 and annular slit 4 formed by insert 5 and nozzle 6. The cross section of the slit is regulated by moving the cone of insert 5 by means of flywheel 7.

As has already been noted, the STS-FOB-2 injector was tested with four additional inserts and five nozzles, to study their effect on the quality of the atomization. The second insert (Fig. 10) differed in that it had four openings 1 to feed a certain amount of air to the base of the fuel jet. The third insert did not differ much from the second except that openings 1 were at 20°, to swirl the air at the base of the fuel jet. In addition, the insert was spherical in shape. The fourth insert differed from the third mainly in its various geometric dimensions.

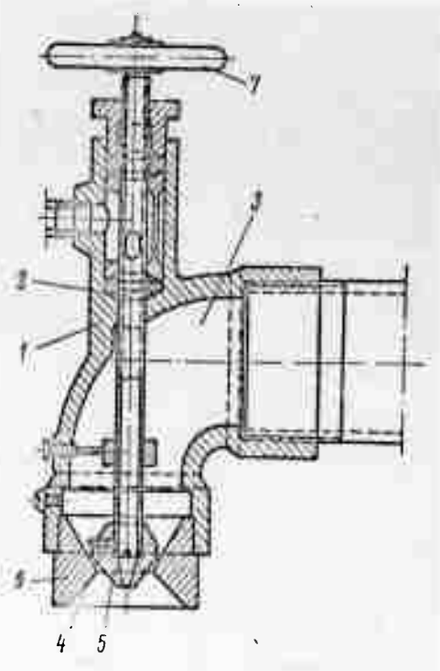

Figure 9. Cut-away view of the STS-FOB-2 (ROMO) injector.

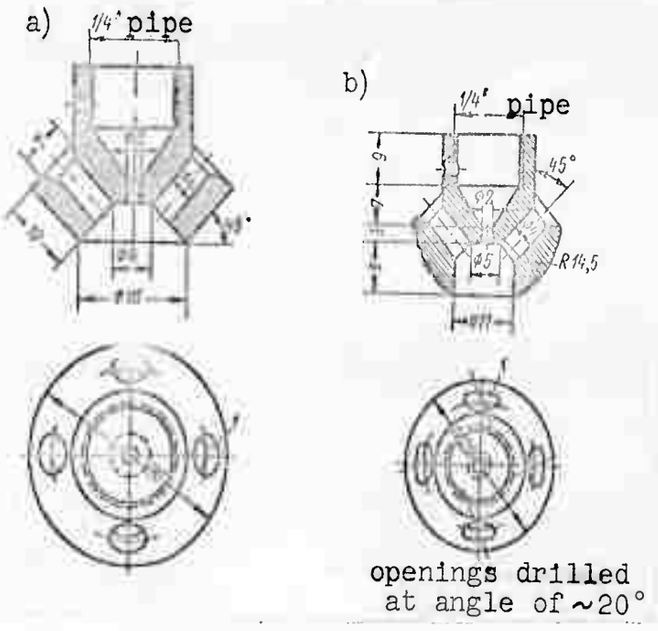

Figure 10. Supplementary inserts for the STS-FOB-2 injector. a- first supplementary insert, b- second supplementary insert.

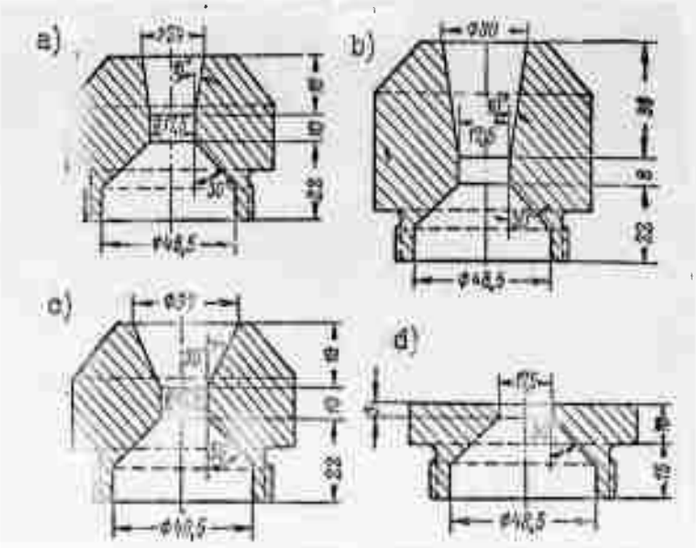

Figure 11. Supplementary nozzles for the STS-FOB-2 injector. a- first supplementary nozzle, b- second supplementary nozzle, c- third supplementary nozzle, d- fourth supplementary nozzle.

The four supplementary nozzles differed from the ordinary nozzle in that after the air meets the fuel, the gas-liquid mixture passes through a straight section, becoming a cone. The nozzles differed among themselves in the length and angle of this cone, and also the length of the straight section. The fifth supplementary nozzle had no straight section, but differed from the basic nozzle in the considerably smaller cone angle. Figure 11 gives the shape and characteristic dimensions of the supplementary nozzles.

The STS-FDM-1 injector, Soyuzteplostroya (All-Union Trust for Design and Construction of Fuel-Burning Equipment and Installations), the Kel'man system (Fig. 12) is designed for a much lower output (from 1.5 kg/hr). The air is fed through tube 1 to the fuel jet

in two paths: the primary air stream goes through annular irregular cross section 2 to the base of the emerging fuel jet, and the second air stream passes through annular slit 4, controlled with the aid of nozzle 3. The fuel passes along central tube 5 and, together with the primary air, passes through nozzle 6 until it encounters the secondary air stream. The fuel flow-rate is regulated by needle-valve 7 by means of flywheel 8.

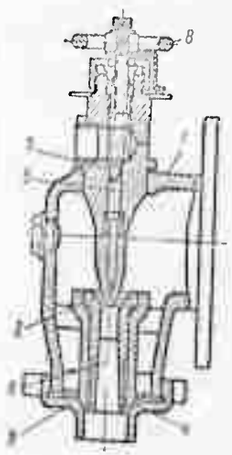

Figure 12. Cut-away of the STS-FDM-1 injector (Kel'man system).

In the Glushakov injector (Fig. 13) the fuel enters tube 2 through tube 1. The cross section of nozzle 3 at the fuel exhaust is controlled by needle 4. This needle moves along a spiral path by means of flywheel 5. The air is fed through pipe 6 to cavity 7, and during the initial opening enters the injector orifice through performations 8 in tube 9. As the flywheel 10 is turned, the advancing edges of tube 9 engage screws 11 and raise bushing 12; additional air enters through the perforations 13 in this bushing. The injector provides for combustion of the gas which is fed through tubes 14 and

openings 15. Ring 16 is intended to control the air drawn in through openings 17.

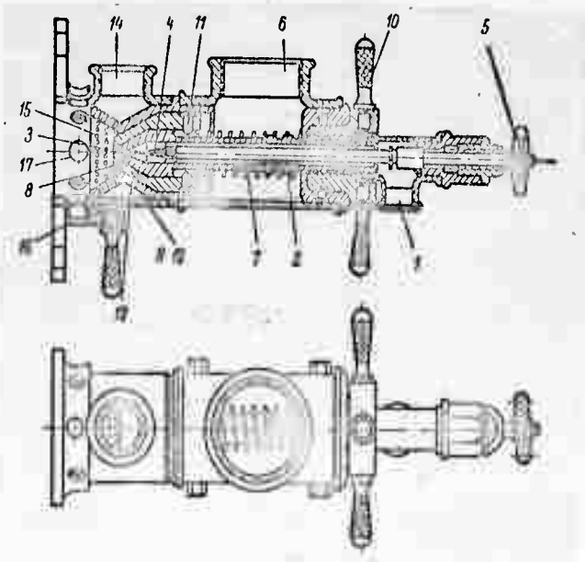

Figure 13. Cut-away of the Glushakov injector.

Figure 14 shows the two-stage injector. In this injector the fuel enters through pipe 1 and channel 2 into tube 3. The fuel flow-rate is controlled by valves 4 and flywheel 5. The air enters the common chamber 6 through tubes 7 and is divided into primary and secondary. The primary air passes through swirler channels 8 to mixing chamber 9. The secondary air enters the injector orifice through annular slit 10 whose size is governed by means of flywheel 11.

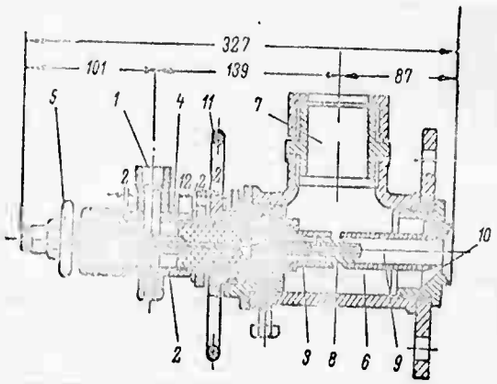

Figure 14. Cut-away of the two-stage injector.

Figure 15 shows the installation for testing industrial injectors. The central part of the stand is a wooden chamber 6, with the injectors to be tested (9) installed vertically in the top. This was convenient for conducting the experiments, thanks to the presence of the axis of symmetry of the atomized jet. The bottom of the chamber was adapted to collect the processed liquid. The air was fed by centrifugal fan 16 and its flow was measured by collar 13 and manometer 14. The air pressure was measured by manometers 12 and 10, and the temperature by thermometer 15. Tap 11 served for more convenient regulation of the air flow and to prevent the fan from overheating with low flow-rates. The fuel from service tank 2 entered injector 9 under a pressure created by compressor 1. The bottom of the service tank contained a tap for liquid run-off. The top contained a funnel for filling, manometer 4 for pressure measurement, and a pocket with thermometer 5 for temperature measurements. The fuel flow was measured using a measuring glass. Heater 3 was used to warm the liquid within the service tank.

Inside the chamber is a frame with lateral guides on which, in the center of the jet, is a strip with graduated cylinders 7 to study the flame density through the diameter of the jet. Six series of guides attached at various heights in the frame, determined the position of the graduated cylinders from the injector orifice. The first guide was 450 mm from the injector. The other guides were 200 mm apart.

Device 8 was used to collect the drops; this is a cylinder with a performation which revolved about a fixed axis. This axis held the slides coated with the basic compound. As the cylinder rotated the slit passed at high speeds over the slides and thus the individual

drops were cut off. The device was placed on the guides of the frame (together with the strip containing the graduated cylinders).

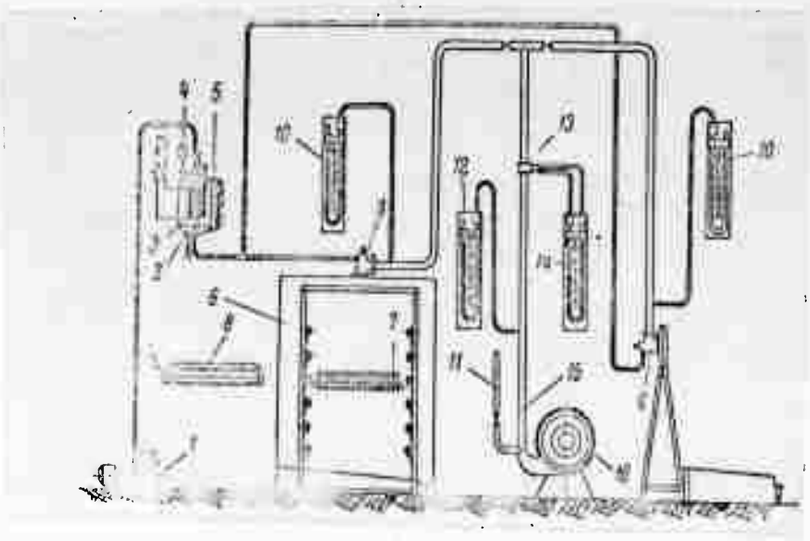

Figure 15. Diagram of the experimental installation for investigating atomization in injectors.

The method of conducting the experiments, as well as the processing, did not differ in principle from those used in the laboratory installation. The coating of the slides was the only exception. In the first series of experiments with the industrial injectors the slides were coated with a layer of castor oil. The industrial injectors, because of the great flow-rates, were tested using water; with a soot coating the drops spread and lost their primary form. To prevent a change in the diameter of the drops because of an increase or decrease in the viscosity of the castor oil and water evaporation, the collected drops, from the moment they were cut off to the moment they were measured, were held in a saturated atmosphere at a constant temperature of approximately 18°C. Later,

the castor oil was replaced by a mixture of vaseline and transformer oil in a ratio of about 1:3. This liquid, developed by A. G. Blokh, retains for a long time the drops which strike it, not allowing them to fuse and evaporate.

The relative speed of the gas-liquid stream, when the primary and secondary air is fed to the injector, was calculated according to the formula

$$w=\sqrt{\frac{w_{10}^2L'+w_{20}L''}{L}}, \qquad (12)$$

where w_{10} is the initial relative speed between the primary air and the liquid jet; w_{20} is the relative speed of the gas-liquid stream when it encounters the secondary air; L' is the flow of primary air; L" is the flow of secondary air; and L is the total air flow.

Description of the Experiments, and the Processing Results

The experiments with all injectors were conducted mainly with their calculated output. The amount of air used and the ratio of the air and liquid flow-rates varied within rather broad limits. The flow-rates of the primary and secondary air were determined from the ratio of the cross sections. Several of the experiments with STS-FDB injectors were conducted only with primary air (complete cut-off of the secondary air).

Figure 16 shows (in logarithmic anamorphism) the functional dependence

$$\frac{d}{D}=f\left(\frac{\rho w^2 D}{\alpha}\right),$$

for all the injectors tested. From Fig. 16a it is evident that the points of all the experiments with the STS-FOB-2 injector, in various modification, i.e., with various combinations of inserts and nozzles,

are practically generalized in a straight line which can be expressed by the equation

$$\frac{d}{D} = A_0 \left(\frac{\rho w^2 D}{\alpha} \right)^{-0,45}. \qquad (13)$$

The other injectors tested (Fig. 16b, c, d, e) have the same dependence.

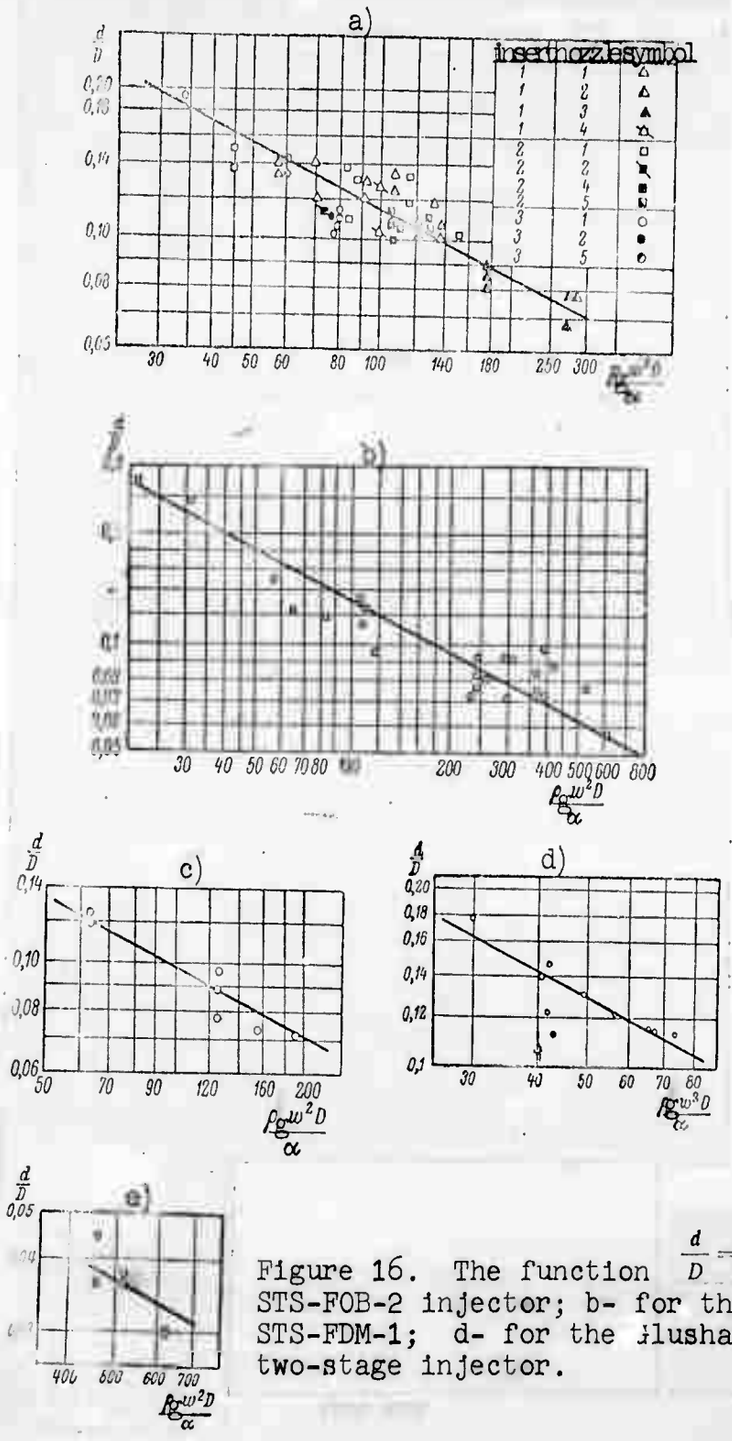

Figure 16. The function $\frac{d}{D} = f\left(\frac{\rho w^2 D}{\alpha}\right)$ a- for the STS-FOB-2 injector; b- for the STS-FDB-1; c- for the STS-FDM-1; d- for the Slushakov injector; e- for the two-stage injector.

Figure 17 gives a comparison of the curves for the four atomizers. A series of parallel lines, inclined toward the abscissa, is obtained in logarithmic coordinates. As the figure shows, for all tested industrial injectors, as for the laboratory types, we have the dependence

$$\frac{d}{D} = A_0 \left(\frac{\rho_g w^2 D}{\sigma} \right)^n,$$

where n is a constant, equal to -0.45. The coefficient A_0 varies for different injectors, and depends on their design. Table 4 gives the values of A_0.

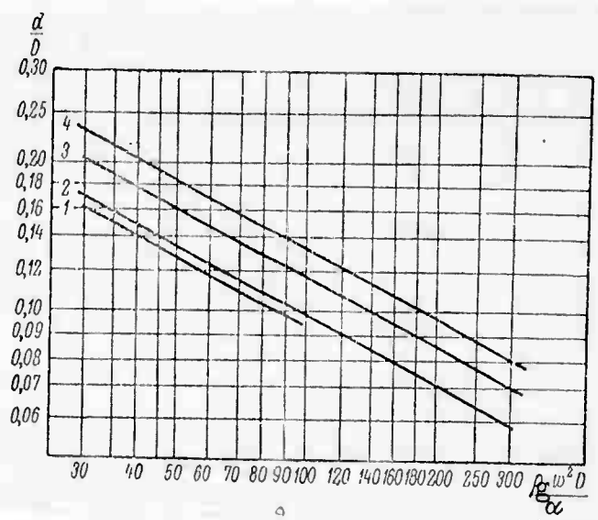

Figure 17. The dependence $\frac{d}{D} = f\left(\frac{\rho_g w^2 D}{\sigma}\right)$ for four injectors. 1- the Glushakov injector, 2- the STS-FDM-1 (Kel'man system), 3- the STS-FOB-2, 4- the STS-FDB-1.

Table 4

Values of the coefficient A_o

Name of injector	A_o
STS-FDB-1	1.20
STS-FOB-2	0.90
STS-FDM-1	0.78
Glushakov	0.75
Two-stage injector	0.61

The distribution of the liquid throughout the jet (spray density) was of the same nature for all injectors, differing only in the width of the flame.

Figure 18 shows the typical distribution of spray density for the STS-FDB-1 for two distances from the nozzle. Here the distance from the center of the jet (0) in millimeters is plotted along the abscissa, and the spray density in percents of total flow is plotted along the ordinate. From the liquid distribution curves it is evident that for the tested injectors, unlike the swirl injectors, maximum density is at the center of the jet, decreasing toward the edges, and that the greater the distance from the injector orifice, the more the flame density in the center decreases with expansion of the jet boundaries and with a relative increase in density at the edges.

Experiments conducted at various distances from the injector orifice made it possible to determine the shape of the jet and the angle of conicity. The shape of the jet is shown graphically in Fig. 19, where the jet width r in millimeters is plotted along the

abscissa, and the distance from the injector h in millimeters is plotted along the ordinate. The figure shows that the jet of liquid emerging from the nozzle is first dispersed in the shape of a cone whose edges, at a certain distance, begin to compress. Such a form of the atomized jet is characteristic of non-swirler air injectors.

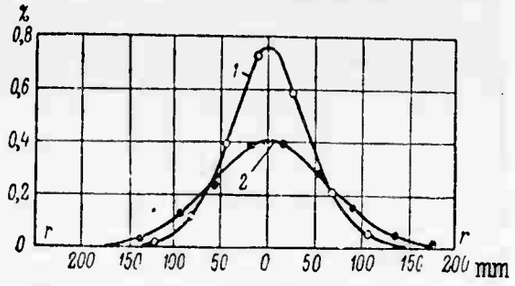

Figure 18. Distribution of the liquid throughout the jet for the STS-FDB-1 injector for various distances from the nozzle. 1- 630 mm, 2- 1030 mm.

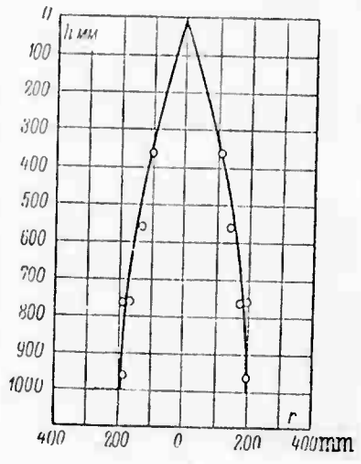

Figure 19. Change in shape of a jet along its length; injector STS-FOB-2, insert 3, nozzle 1.

The numerical values of the angles of conicity for the test

injectors are given in Table 5, which shows that the STS-FDM-1 has the smallest angle, the STS-FOB-2 the greatest.

Table 5

Angles of conicity of injectors

injector	insert number	nozzle number	angle of conicity
STS-FDB-1	—	—	28
STS-FOB-2	1	1	30
The same	1	2	32
"	1	3	34
"	1	1	36
"	1	2	32
"	1	4	31
"	3	5	37
"	3	1	33
"	4	5	37
"		6	47
STS-FDM-1 (Kel'man)	—	—	22
Glushakov injector	—	—	25
two-stage injector	—	—	29

The tests conducted made it possible to make a number of remarks on the designs of individual injectors.

1. The STS-FDB-1 injector has relatively complex design. We cannot consider it justified that this injector has a slide valve, carefully processed mechanically, enclosed in cast iron. This can serve only as a stop valve. Attempts to use it to regulate the total air-flow were completely unsuccessful, since with partial closure the jet was beveled, and the hydrodynamic regime was made worse. Considering that in practice an air valve is installed ahead of each injector, in order to switch it out if necessary, it is best to produce such injectors without special slide valves. It must also be mentioned that under the test conditions it was impossible to feed

the STS-FDB-1 injector with air having a pressure greater than 400 mmHg (limiting the fan). However, the obtained data make it possible to compare the operation of this injector with others, and also, using formula (13), to determine, approximately, the nature of its operation under rated conditions (450-700 mmH_2O).

2. The tests have shown that a change in the basic parts of the ROMO injector has no appreciable effect on the atomization quality. In the final choice of certain inserts or nozzle we must proceed from specific operational conditions as, e.g., air pressure and angle of conicity. It should, however, be pointed out that nozzle No. 3 in combination with insert No. 2 should be rejected as not satisfying the basic requirements of the injectors, since incorrect ratios of the geometric dimensions lead to the formation of a film during atomization. Such a film also forms during operation with insert No. 4 and Nozzle No. 6 because of the small angle of solution of the cone of the nozzle. The formation of a film was often noted during operations with insert No. 2, the use of which is also undesired. It is also undesirable to use air swirling as is done with inserts Nos. 3 and 4. The hydraulic resistance of an injector with insert No. 4 and nozzle No. 6 is somewhat less than in other variants, which made it possible to obtain higher speeds with an identical air head. It is to be expected that with selection of the proper angle at which film formation on the nozzle will be eliminated, and with creation of corresponding swirling in the insert, better results will be obtained in comparison with the basic design (insert No. 1 with nozzles Nos. 1, 2, and 3).

3. The STS-FDM-1 injector (Kel'man system) is highly flexible, operating within broad changes of output. Its basic advantages also

include its extremely simple design, satisfactory operation with extremely low fuel flow-rates, and its better atomization, compared with the other tested injectors, at low air pressure.

4. It should be mentioned that in the Glushakov injector, when the fuel flow was regulated by the needle, the flame was beveled and traced the turning of the needle. This was probably due to incorrect needle design. The needle moved by means of screwthreads, which resulted in a shift of the centering and a skewing of the stream. It would be more correct to set up the controls using a gradually moving needle.

5. The two-stage injector is relatively complex to produce and has no advantages over the other types. During the operation of this injector we observed the formation of large drops which periodically tore loose from the nozzle. Evidently, this was the result of incorrect configuration of tube 9 (Fig. 14), having no expanding part, which caused the liquid to strike the wall, form a film, and be torn away by the air stream in the form of large drops.

3. Determination of the Degree of Uniformity of the Drops

An important factor in the operation of atomizers is the degree of uniformity of the drops, i.e., their distribution by sizes.

Figure 20 shows the discrete diameters of drops δ, plotted along the abscissa, and the percentage weight of the liquid consisting of drops larger than δ, plotted along the ordinate. The three curves in the figure correspond to identical experiment conditions, but different relative speeds. Curve 1 corresponds to more uniform atomization than curves 2 and 3.

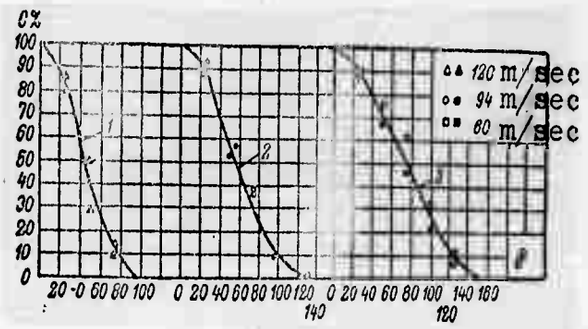

Figure 20. Curves of the distribution of liquid by drop sizes. 1) w = 120 m/sec; 2) w = 94 m/sec; 3) w = 60 m/sec.

Assuming that the distribution of drops by sizes is determined by the law of probability, we get the familiar formula, derived for the case of the pulverization of solid fuel:

$$R = e^{-\left(\frac{1}{m}\ln\frac{\delta}{d}\right)^m}, \qquad (14)$$

where R is the part, by weight, of the liquid consisting of drops whose sizes exceed δ; d is the mean drop diameter; and m is a constant which depends on the injector design, and determined from experiments.

The value of the constant m describes the degree of uniformity of the drops: the greater m, the more uniform in size are the drops.

Figure 21 gives the function

$$R = f\left(\frac{\delta}{d}\right). \qquad (15)$$

for a laboratory injector. From the figure it can be seen that the experimental points for all regimes and liquids are satisfactorily connected by one curve.

The constant m can be determined if we take the logarithm of the quantity 1/R two times.

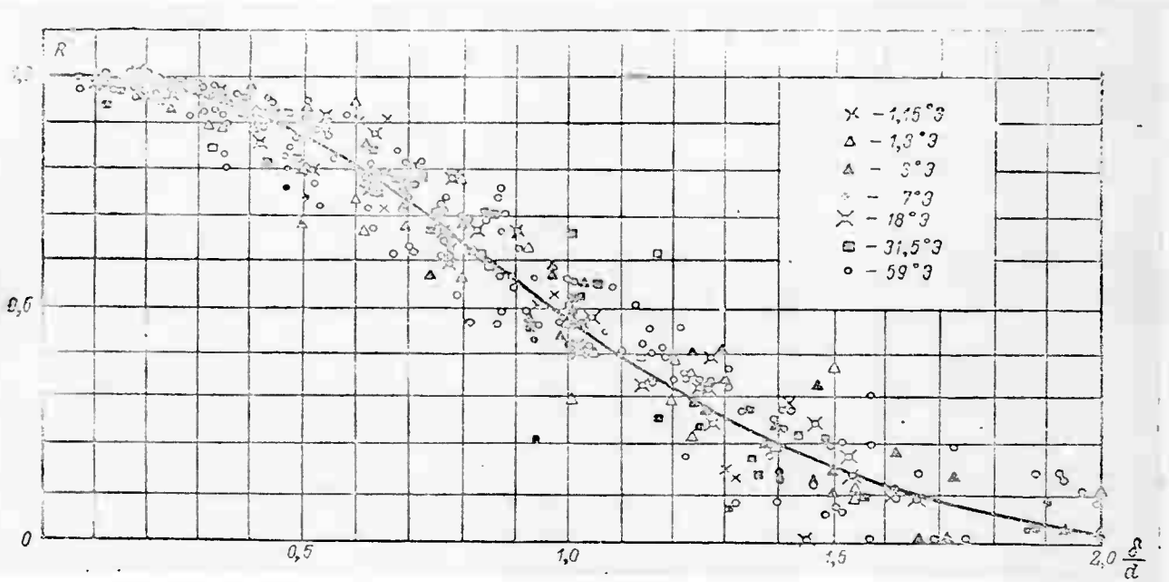

Figure 21. The function $R = f\left(\frac{\delta}{d}\right)$ for a laboratory injector.

The functions $R=f\left(\frac{\delta}{d}\right)$ for the other injectors have a form analogous to that shown in Fig. 21, but with differing values of the coefficient m.

Table 6 gives the values of m for the tested injectors.

Table 6

Values of m for injectors

Injector	m
laboratory injector	2.3
STS-FDB injector	2.8
STS-FOB-2 injector	2.6—3.0
STS-FDM-1 injector	2.8
Glushakov	2.3
two-stage injector	2.8

As Table 6 shows, the laboratory and the Glushakov injectors have the least uniformity. All other tested industrial injectors give distributions of drops close in size.

Conclusions

1. The application of the theory of similitude to problems of the atomization of a viscous liquid in air injectors has resulted in a criterial function for determining the mean diameter of the drops of an atomized jet:

$$\frac{d}{D}=f\left(\frac{\rho_a w^2 D}{\sigma};\ \frac{\mu^2}{\rho_l \sigma D}\right).$$

2. Experiments conducted on a laboratory installation with viscosity changes from 1 to 60°E and a coefficient of surface tension

from $2.4 \cdot 10^{-3}$ to $7.2 \cdot 10^{-3}$ kg/m, gave a function expressed by formulas (9) and (9') within limits of a change in the criterion $\frac{\mu^2}{\rho g a D}$ from $4.5 \cdot 10^{-5}$ to 7.25 and values of $\frac{d}{D} \cdot \left(\frac{\rho w^2 D}{a}\right)^{0,45}$ from 0.77 to 2.4.

3. We found no change in the fineness of atomization along the jet. To determine the length of the section in which atomization is accomplished we must use another method, making it possible to study the quality of atomization in the immediate vicinity of the injector orifice.

4. We have given recommendations for the regime characteristics and evaluated the quality of the injectors, and also indicated several design changes for the test injectors.

5. The degree of uniformity of the drops (size distribution) can be determined by using the formula

$$R = e^{-\left(\frac{1}{m}\,!\,\frac{\dot{l}}{d}\right)^m},$$

where m is a constant which depends on the injector design.

REFERENCES

1. LOS'KOV, D. N. in the collection: Materialy po ekonomii topliva v pechakh (Data for conserving fuel in furnaces), edited by N. N. Dobrokhotov. NIIMASh (Scientific-Research Institute of Machinery and Metalworking), 1938.

2. BOGOMOLOV, D. I. Orginformatsiya (Organizational Information), OBTI, 11, 1931.

3. KOPYTOV, V. F. Neftyanyye forsunki nizkogo davleniya (Low-pressure petroleum injectors), Ural'skaya Metallurgiya (Ural Metallurgy), 9-10, 1938.

4. KOPYTOV, V. F. Zhurnal NIIMASh (Journal of the NIIMASh), No. 8, 1934.

5. KATS, V. Ya. Ispytaniya forsunok Orgenergo (Tests of the "Orgenergo" injectors), Byulleten' Orgenergo (Bulletin of the All-Union Trust for Improving the Efficiency of Power Systems and Fuel Supplies), 4, 1937.

6. EFROS, M. M. Issledovaniye raboty neftyanykh forsunok nizkogo davleniya (Study of the operation of low-pressure petroleum injectors), Trudy Konferentsii po Promyshlennym Pecham (Transactions of the Conference on Industrial Furnaces), VNITOE (All-Union Scientific, Engineering and Technical Society of Power Engineers), 1949.

7. PLEKHANOV, V. G. and SIMONOVA, T. I. Vestnik Metallo-promyshlennosti (Herald of the Metal Industry), Nos. 7 and 9, 1933.

8. RAMZIN, L. K. Izvestiya VTI (News of the All-Union Heat Engineering Institute), 2, 1927.

9. TRIBING, G. Injection in Diesel Engines, Vienna, 1925.

10. RAYLEIGH, S. Proc. of the Royal Soc. of London, XXIX, 1879.

11. WEBER, K. Internal combustion engines, ONTI (Joint Scientific and Technical Press), 1936.

12. KATSNEL'SON, B. D. and SHVAB, V. A. Issledovaniye protsessov goreniya natural'nogo topliva (Study of the combustion of natural fuel), collection edited by G. F. Knoppe, Gosenergoizdat (State Power-Engineering Press), 1948.

13. NATANZON, V. Ya. Dizelestroyeniye (Diesel Engineering), Nos. 3-5, 1938.

UNCLASSIFIED